SEARCH: SEgmentation of polaR Coronal Holes

Ajay Kumar Tiwari[1], Benoit Tremblay[2,3,4], Andong Hu[1], Linnea M. Wolniewicz[3], Michael Kirk[5,6], Silvina Guidoni[7], Brent Smith[8], Matthew Penn[9], Tanmoy Samanta[10]

[1]Centrum Wiskunde & Informatica, NL - [2]Laboratory for Atmospheric & Space Physics, USA - [3]CU Boulder, USA - [4]National Solar Observatory, USA - [5]ASTRA, USA
[6]NASA Goddard Space Flight Center, USA - [7]American University, USA - [8]Johns Hopkins Applied Physics Laboratory, USA - [9]NVIDIA, USA - [10]George Mason University, USA

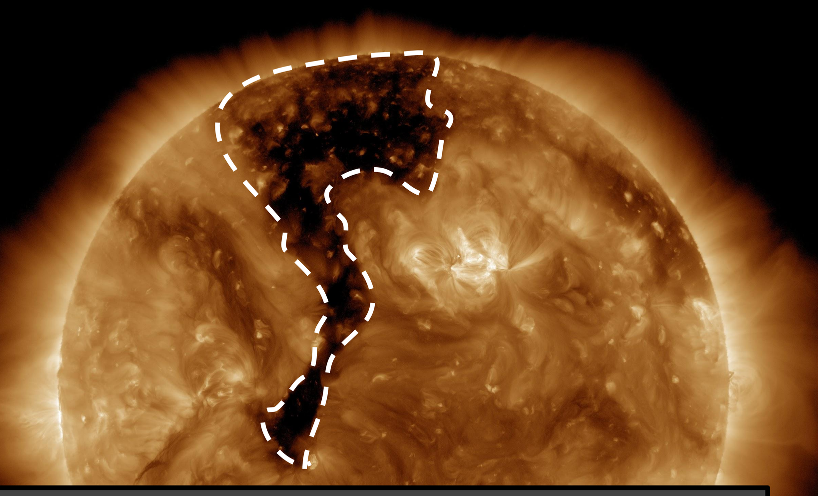

1. Introduction to the Sun's Coronal Holes

- **Solar coronal holes (CH)** are dark regions observed in images of the Sun taken in extreme ultraviolet (EUV) and soft X-ray wavelengths (**Figure 1**). CHs correspond to magnetic field lines (represented with white lines in **Figure 1**) that originate at the Sun and extend to interplanetary space (*open* field).
- Polar regions of the Sun are of special interest for space weather because they are the sources of high speed solar wind towards the Earth and other planets [1, 2, 3], but they remain elusive to the current constraints of solar imagery. **Indirect methods are needed for understanding the polar environment, including polar CHs.** Polar magnetic fields are used to forecast upcoming solar magnetic activity cycles [4, 5].
- The identification of CHs has been done traditionally with intensity-based thresholding methods applied to Sun images. Recent advances include supervised machine learning (ML) methods [6, 7].
- **In this work, we use EUV data from the three vantage points (*e.g.*, Figure 2a) combined into full-Sun synchronic maps (*e.g.*, Figure 2b) to segment polar CHs (Figure 3). We address the identification of CHs using *unsupervised* learning (clustering and convolutional neural networks), *i.e.* without the use of models or databases and the biases they may have.**
- Through unsupervised learning, we also identified **active regions** (ARs; **Figure 1**), typically associated with closed, confined magnetic field lines. Solar flares and coronal mass ejections, the main drivers of space weather, originate in ARs.

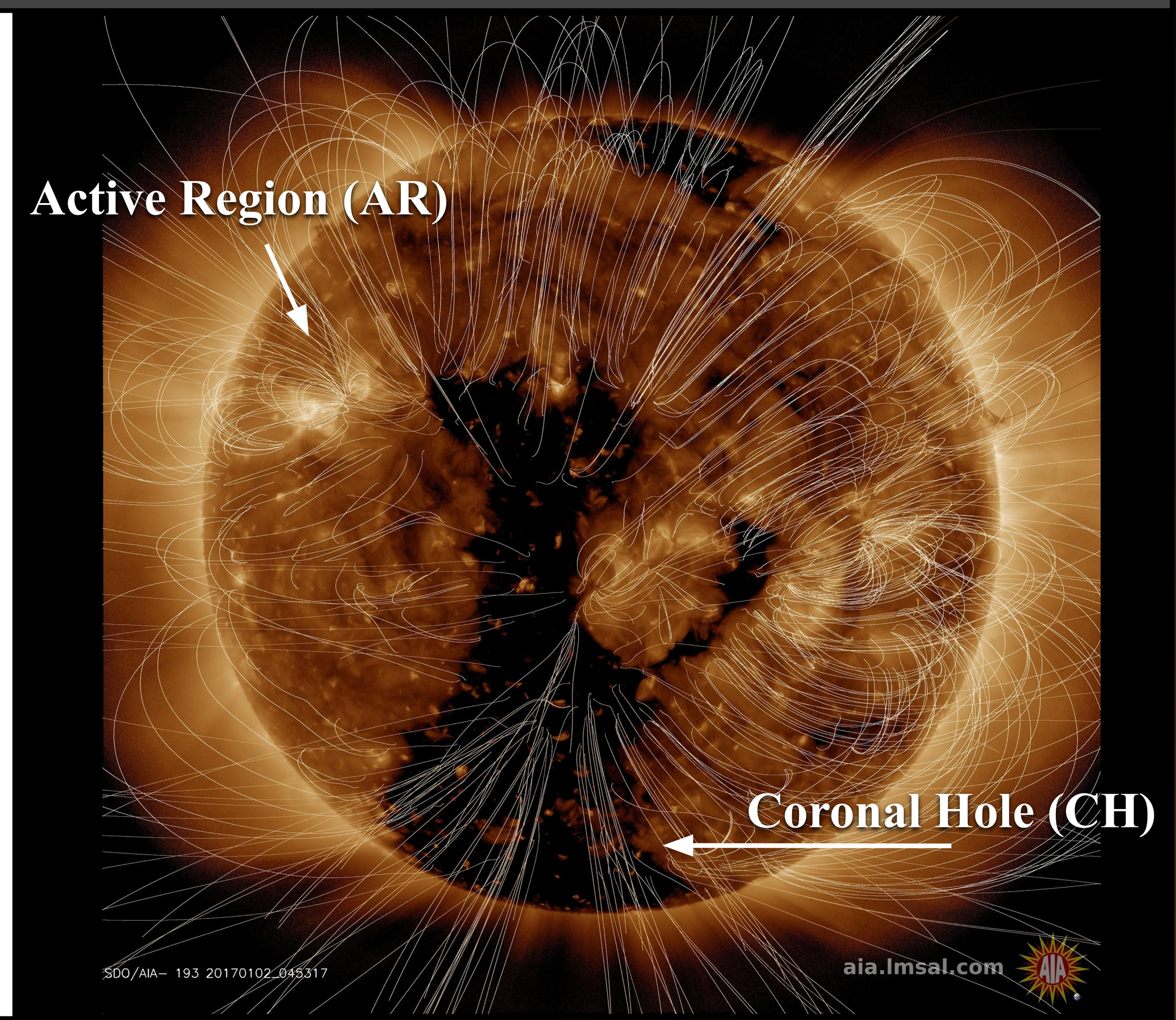

Figure 1: Full-disk image of the Sun captured at a EUV wavelength of 193Å by the Atmospheric Imaging Assembly (AIA) onboard the Solar Dynamics Observatory (SDO).

2. Synchronic Maps: Mapping the Full Sun to Segment Polar Coronal Hole Boundaries

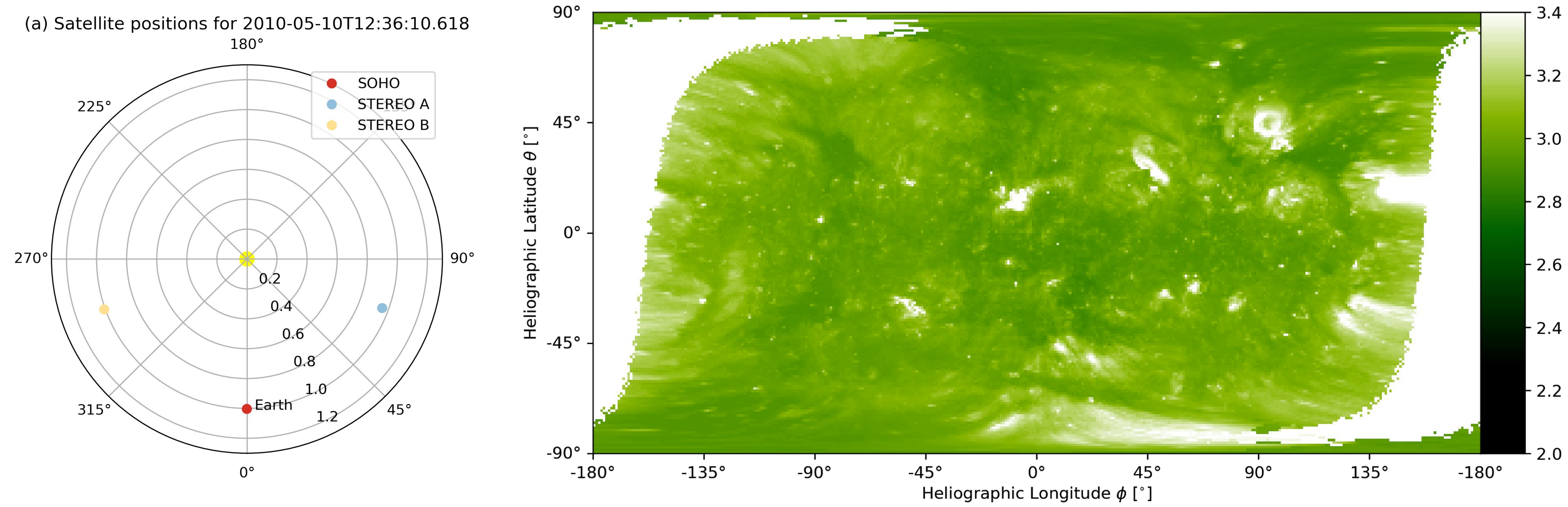

Figure 2: (a) Position of the Solar and Heliospheric Observatory (SoHO) and Solar Terrestrial Relations Observatory Ahead (STEREO-A) & Behind (STEREO-B) satellites on 2010-05-10. (b) **Synchronic maps:** The combination of simultaneous multi-stereoscopic EUV images of the Sun (captured at 195Å by SoHO, and STEREO-A & -B). The white spaces at the two ends of the map show the regions of the Sun that were not covered by any instrument at the time of observation.

3. Using Unsupervised Machine Learning for the Segmentation of (Polar) Coronal Holes in Synchronic Maps

Click for animated version

CH detection methods are limited to existing catalogues and methods as there is no objective way to define CH boundaries. The intersection over union metric (IoU) and the structural similarity index (SSIM) were used to measure the accuracy and the similarity of unsupervised learning with respect to existing CH detections.

Figure 3: Comparisons of three CH detection methods using single-wavelength synchronic maps from the Predictive Science Inc. (PSI) database (colored background). **CHs are shown in yellow and magnetically active regions (ARs) in magenta.**

(a) **PSI CH detections using the EZSEG region-growing-style method** (not machine learning!) [8]. **Reference** to evaluate IoU and SSIM of unsupervised learning methods**.**

(b) **K-means clustering technique** trained to identify 6 clusters, *i.e.* the optimal number computed by the Elbow method [9]. Average SSIM=0.96, IoU=0.60.

(c) **W-net convolutional neural network** [10, 11], with a fully-connected conditional random field (CRF) mask to smooth the segmentation maps. Input images and reference CH masks were downsampled by a factor of 10 in each spatial dimension for memory considerations. No optimization was performed. Average SSIM=0.95, IoU=0.53.

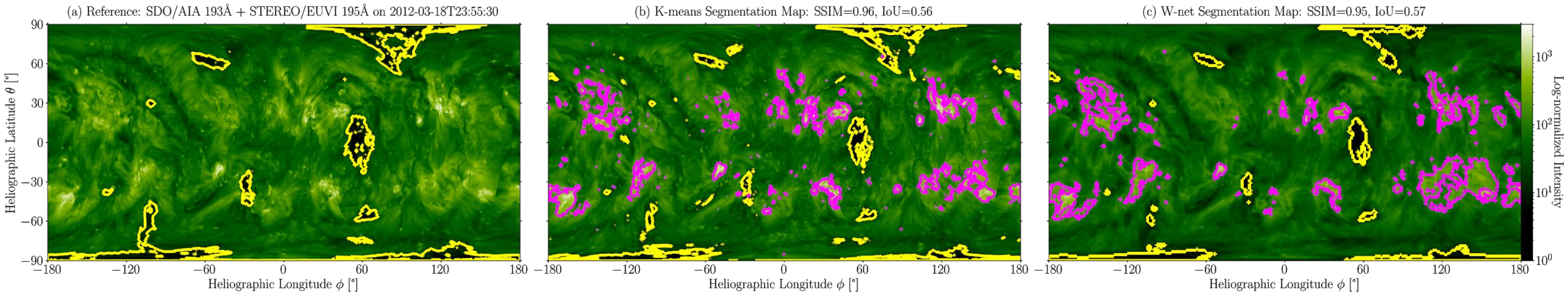

4. Science Application: Correlation between Polar Magnetic Field Strength and Coronal Hole Area

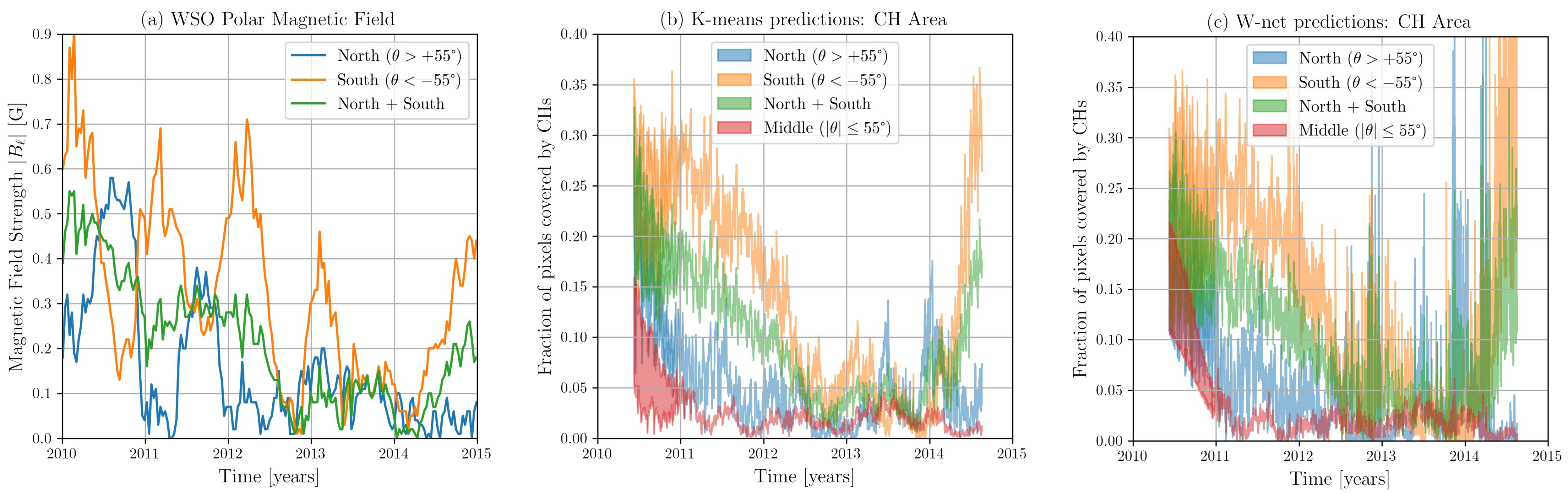

Figure 4: Correlation between magnetic field strength at the Sun's poles (latitude $|\theta| > 55^{\circ}$) and area of polar CHs (fraction of pixels that were labeled as CHs in the same time window). (a) Magnetic field strength from the Wilcox Solar Observatory (WSO). (b) Area of polar CHs computed using K-means. (c) Area of polar CHs computed using the W-net. For each pole, the lower curve assumes that there are no CHs where data is unavailable (lower limit) and the upper curve assumes that all unavailable data belong to CHs (upper limit). **Conclusion: CH size measurements appear to be a good proxy for long-term changes in polar fields**, but more work is needed to causally link the two phenomena.

5. Conclusion & Future Work

In conclusion:

- Unsupervised segmentations provides an **unbiased** way of identifying coronal holes and additionally active regions, two of the most important features for space weather applications.
- The coronal holes identified are consistent with the existing detections [8].
- Preliminary analysis of the magnetic field strength and the polar coronal hole area follows similar trend observed in previous studies [12].

Future work:

- Provide a catalogue of multi-wavelength synchronic maps (SoHO + STEREO) and use those synchronics map to identify and study coronal hole boundaries.
- Optimize the W-net convolutional neural network for solar images.
- Study the relationship between coronal hole area and geomagnetic activity at L1.
- Explore the relationship between the solar cycle and coronal hole area using EUV images captured by SoHO over a full 22- year magnetic cycle.

References

[1] Nolte et al., 1976
[2] Harvey and Sheeley, 1978
[3] Wang and Sheeley, 1990
[4] Schatten et al., 1978
[5] Pesnell and Schatten, 2018
[6] Illarionov & Tlatov, 2018
[7] Illarionov *et al.*, 2020
[8] Caplan *et al.*, 2016
[9] Joshi & Nalwade, 2013
[10] Xia & Kulis, 2017
[11] Rajendrakumar Gare *et al.*, 2020
[12] Cranmer, S. R, 2009

Acknowledgements

This project was first conducted as part of the NASA HelioHackweek 2020. The authors would like to thank their fellow SEARCH team members Emily Mason, Jake Strang, Jamie Staeben, and Luisa Capannolo for their participation, the organizers of HW20 at NASA and at the NASA Center for Climate Simulation, and the team at NVIDIA for their support.